Pre-Study of Graphene-Enhanced Cementitious Materials

Tang Luping, Division of Building Technology, Chalmers University of Technology

Johan Liu and Nan Wang, Laboratory of Bio-Nano System, Chalmers University of Technology

Lilei Ye, SHT Smart High-Tech AB

1. INTRODUCTION

Cement-based concrete is the most widely used building and construction material in the world. Although concrete itself is relatively durable when used under the mild environments, its intrinsic weak tensile strength greatly limits its application due to its porous structure. Traditional strategies to overcome this weakness of concrete include utilization of various reinforcing materials, such as steel bars[1], steel fibers[2], carbon fibers[3], polymer fibers[3–6] and mineral fibers[7,8]. However, some challenges raised from materials themselves limited their applications. For example, steel reinforcement suffered the corrosion problem caused by carbonation or chloride ingress. Polymer fibers have good tensile strength but poor reliability. Large amount of addition of fibers into concrete could significantly decrease the workability of concrete. Previous strategies are basically modifying concrete at macro level without changing the microstructure of concrete, which is quite essential for a high mechanical performance. Mechanical strength of concrete is mainly contributed by the hardened cement paste. During the cement hydration process, the formation of calcium silicate hydrate (C-S-H) gel acts as adhesive and offers the original mechanical strength of concrete. Therefore, the shape and density of the C-S-H gel plays key roles in determining the mechanical properties of the concrete. Seeking a method that can significantly improve the strength of hardened cement paste through regulation of its microstructure is certainly worth considering.

To be able to regulate the microstructure of cement paste, reinforcing materials need to possess some properties including intrinsically high strength, large surface areas, good dispersability in water, and the ability of forming chemical bonds with the C-S-H gel. Traditional materials are hard to fulfill such requirements. However, with the development of nanotechnology, many nanomaterials have been synthesized, such as silica nanoparticles[9], carbon nanotubes (CNTs)[10] and graphene[11]. Among variety of those materials, Graphene oxide (GO), as a graphene derivative, has demonstrated a great potential on the application of cementitious materials due to its high specific surface area, ultrahigh strength and flexibility. Importantly, GO can be easily dispersed into water to form stable dispersions and also able to form composites with polymer and ceramic materials due to existence of large amount of oxygen functional groups.

Inspired by its special structure and superior application properties, GO, as the reinforcing material, was utilized to refine the microstructure of cement in this project. To improve the bonding between GO and C-S-H gel, necessary surface treatment of GO has been carried out, such as surface coating with silica layer or other inexpensive oxides, surface functionalization with silane groups to form covalent bonds with C-S-H gel. Morphology analysis of the functionalized GO materials (fGO) was performed and identified the existence of functional materials. A modified mixing process was also developed for uniformly dispersing fGO with cement paste mixture. Mechanical tests indicate the reinforcing effect of fGO to concrete. Moreover, microstructure comparison of concrete samples with different amounts of fGO addition reveals that the shape and density of the C-S-H gel are able to be regulated by adding certain amount of fGO and lead to a decreased porosity in hardened cement paste. Similar results can also be reflected from the density measurement, in which the fGO reinforced concrete shows a higher density than the reference one. All these results in the pre-study indicate the great potential of fGO in the aspect of improving mechanical properties of concrete.

2. RESEARCH BACKGROUND AND BASIC IDEAS

2.1 The atomic structure of C-S-H hydrates

To further understand the mechanism of cement hydrates making bonds with the graphene, it is crucial to investigate the hydration of cement. After mixing the cement powder with water, a myriad of chemical reactions happen and a rigid, complicated and porous material is formed, called cement paste.

Actually, the cement paste can be also described as a composite material consisting of amorphous C-S-H gel, calcium hydroxide crystals (portlandite), aluminates and non-hydrated cement. The C-S-H gel dominates the most important properties of hardened cement paste.

Several models have been proposed to describe the C-S-H gel's nanostructure. C-S-H may have a crystalline structure similar to the tobermorite and jennite crystals (Figure 1). Some studies stated, however, that C-S-H could have an amorphous [12] or crystalline structures[13].
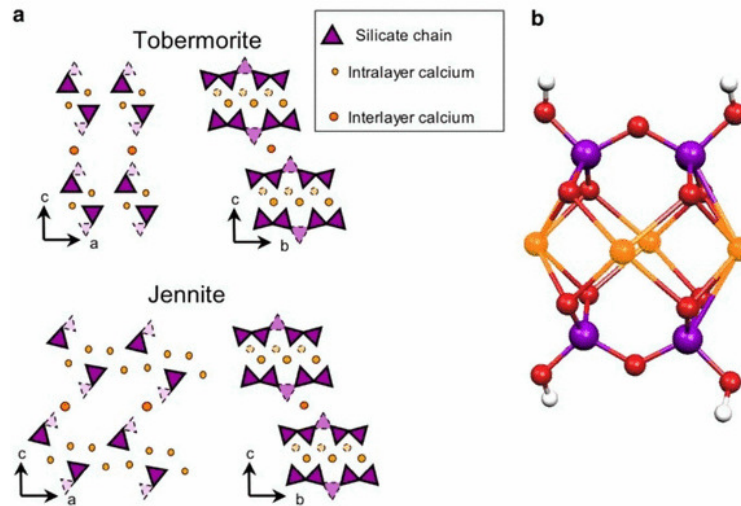
Figure 1 Atomic models of the tobermorite and jennite crystals.

There are more than 30 different crystalline structures mainly represented by the 14-Å tobermorite and jennite. The amorphous gel structure is very difficult to model. C-S-H gel is often referred with its Ca/Si ratio, which varies between 0.7 to 2.3. This high variability explains the reason why the extensive research conducted so far has not given a precise picture of the C-S-H nanostructure or how we could reinforce and enhance its properties. Besides that, the chemical composition varies within the cement paste. Thus, in order to investigate the nanostructure of C-S-H, more parameters need to be investigated such as: the variations of the Ca/Si ratio, silicate structure, and contents of Si-OH and Ca-OH [14].

Tobermorite has Ca/Si ratio of 0.83 and density of 2.18 g/cm^3, whereas Jennite has Ca/Si ratio of 1.5 and density of 2.27 g/cm^3. Richardson introduced two models for the C-S-H gel's structure: the tobermorite/jennite (T/J) models and the tobermorite/calcium hydroxyl (T/CH) models[15]. In addition, Richardson suggested that the C-S-H gel structure may have glass-like and crystalline properties due to the mineral tobermorite. The atomic structures proposed were: 14-Å $Ca_5Si_6O_{16}(OH)_2 \cdot 7H_2O$ for tobermorite and $Ca_9(Si_6O_{18})(OH)_6 \cdot 8H_2O$ for jennite.

The scanning tunneling microscope (STM) showed that the shape of C-S-H resembles disks of 5 nm thickness. During the hydration phase, C-S-H gels are classified in two categories depending on their density: (HD) High Density C-S-H gels and (LD) Low Density C-S-H gels, which also have different mechanical properties. The ratio of high density to low density C-S-H gels depends on the design of the mixture.

Jennings suggested that C-S-H gels have a colloidal structure with different packing densities. Increase in the packing densities means higher number of contacts between the particles of the cement paste. The HD C-S-H gels have greater stiffness and hardness due to the fact that they have more contacts between the particles.

2.2 The atomic structure of graphene and GO

Graphene originally comes from single-layer carbon atoms well-packed in a 2D honeycomb

lattice and is the main element for the synthesis of all the other graphitic materials of all dimensions. It can be found closed in 0D fullerenes, wrapped in 1D nanotubes or stacked in 3D graphite[16], as shown in Figure 2.
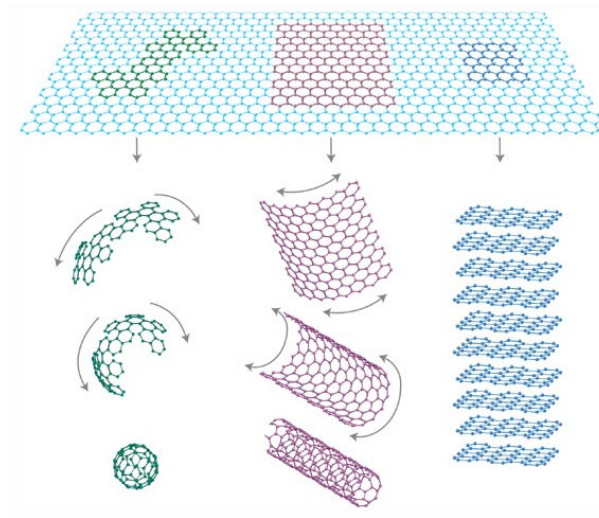

Figure 2 Graphene as a 2D building material for carbon materials of all types of dimensions.

The atomic structure of graphene can be easily understood if the elemental carbon and its 3D allotropes are studied. The atom of carbon has atomic number 6, which means that its atomic orbitals are: $1s^2$, $2s^2$, $2p_x^1$ and $2p_y^1$. The atom of carbon is tetravalent, which means that only the four exterior electrons participate in covalent bonds.

Figure 3 shows the atomic orbital diagram of a carbon atom at ground state (case a) and later on hybridized to sp^3 form (case b) of the diamond and the hybridized sp^2 form (case b) of the graphite and graphene[17].
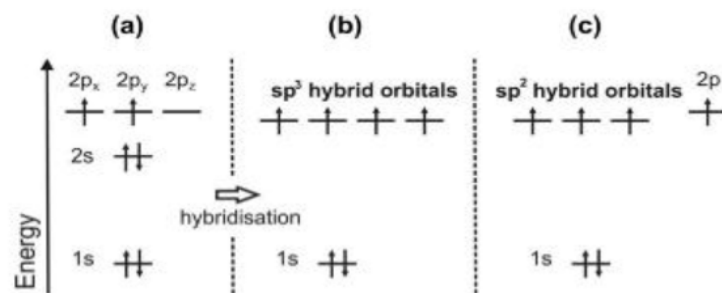

Figure 3 The atomic orbitals of carbon element.

Graphene is a 2D layer material, has one atom thickness, sp^2 covalent bonded carbon atoms, which form a honey-comb crystal lattice. The intrinsic strength of graphene is 130 GPa and its Young's modulus is 1TPa according to atomic force microscopy (AFM) for a single layer graphene sheet. Graphene's planar structure is beneficial for bonding on the upper and bottom surface in close distance with the hosting material. The theoretical specific surface area of a single sheet of graphene could be 2630 m^2/g, which is even higher than that of carbon

nanotubes. The bigger the surface area is, the more possible it becomes to interact physically and chemically with the host material and enhance the bonds formed between these two materials. Although, graphene is extremely attractive due to its remarkable properties, there is significant difficulty to produce more than small quantities and lower the cost of production in order to facilitate its massive production and industrial application.

For this reason, GO, which is a graphene derivative, has been examined as an alternative nanomaterial to graphene. GO is also a single layer material of sp^2 hybridized carbon atoms derivative by a mixture of hydroxyl and epoxy functional groups. Figure 4 shows the GO structure with its oxygen, hydroxyl and carboxyl functionalities above and under the basal plane according to Lerf 's schematic model[18].
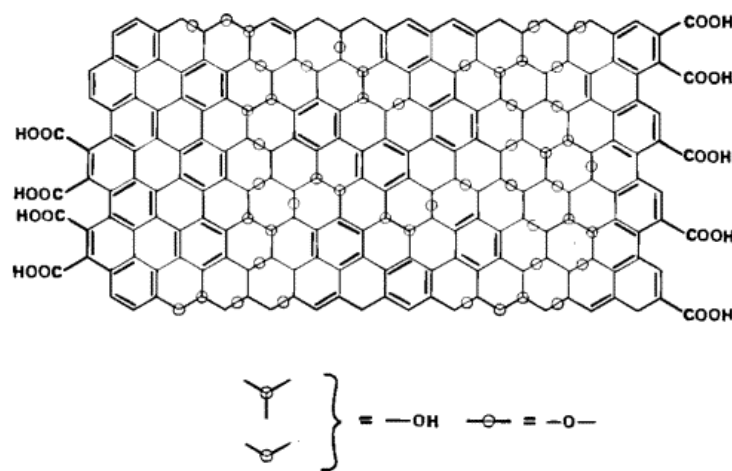

Figure 4 GO structure with its oxygen, hydroxyl and carboxyl functionalities

2.3 Morphological relationships between the fresh cement paste and graphene

Well-dispersed graphene and good interfacial interactions between the graphene nanoparticles and the cement matrix are essential for obtaining increased mechanical and physical properties of concrete.

It is difficult for graphene and other graphite nano-materials to be well-dispersed into the cement matrix, since the cement particles are in the micro-scale in an aqueous solution (Figure 5). The hardened cement paste includes micro- to nano-sized pores, which also limit the contact surface area of graphene with the cement hydrates. Graphene and other graphite nanomaterials could take the space between the micro-sized particles of the cement paste. To achieve thorough dispersion in the cement matrix, micro-scale cement particles could be partially replaced by silica fume nano-particles. In this way, the particle size distribution would be improved and uniform dispersion would be achieved.
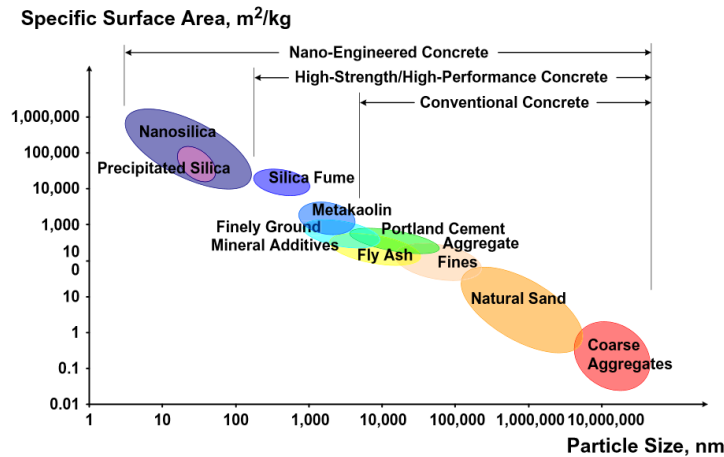
Figure 5 Particle size and specific surface area related to concrete materials.

During hydration, the cement particles react with water and conceive partially the space between them. The rest space is occupied by micro-scale capillary pores formed. The hydrated cement consists of C-S-H gels (where the main binding force between them is Van der Waals bonds), micro-scale C-H crystals, other hydration products, and capillary and gel pores.

The water-cement ratio affects the amount of capillary pores in the hydrated cement paste. In addition the specific surface area of calcium hydroxide micro-scale C-H crystals is smaller than the other hydration products, thus their ability to make bonds with graphene is limited. Hence, the presence of micro-scale pores and crystals limits the interaction of graphene and hydrated cement gels.

Better particle size distribution of the fresh cement mixture and the use of superplasticizers (surfactants) to increase the workability of the cement mixture with the use less water (thus less capillary pores) would refine the micro-morphology of the hardened cement paste and also improve graphene's reinforcement efficiency .

Functionalization of graphene and its derivatives could improve their compatibility with the cement hydrates, forming stronger chemical bonds. Functionalized graphene could benefit both its dispersion in aqueous solution and the interfacial bonds with the cement hydrates. However, functionalization techniques should be further improved in order not to excessively damage the graphene's structure.

2.4 Graphene functionalization

Among the fabrication methods of graphene, GO is widely used as starting material due to its good dispersion, bulk production and unique multifunctional properties.

When graphene is produced from GO, it is already functionalized but the residual oxygen-containing functional groups are not enough to maintain the surface area needed for stable dispersion in the solvents. For this reason, GO's surface should be further modified in

order to be well-dissolved and also have better interfacial interaction with the cement hydrates.

Graphene can be functionalized with three different methods; each one having advantages and disadvantages:

1) Non-covalent attachment of large/small aromatic-containing molecules through π-π stacking

⊕ There is no high damage because of the functionalization.

⊖ Weak bonds are developed, thus the load bearing capacity of the composites is quite low.

2) Grafting molecules on the basal plane of graphene

⊕ Strong bonds are created between graphene and the attached molecules

⊖ Defects are introduced on the graphene surface, thus the graphene's structure weakens

3) Chemical reactions between the functional groups on GO and other molecules, together with subsequent or simultaneous chemical reduction

⊖ Not suggested method for graphene produced by thermal exfoliation (>550°C)

The residual functional groups attached to the GO's surface, such as hydroxyl, epoxy, carbonyl, carboxylate groups, etc. could react with other functional groups grafted on the desirable molecules. This method doesn't harm the graphene structure and provides higher thermal stability than grafting molecules on the basal plane of graphene.

In another research study, Petrunin et al. investigated the performance of cement composites with functionalized multi-walled carbon nanotubes[19]. The multi-walled carbon nanotubes were functionalized with carboxylic groups by grafting on their surface. The compressive strength test results showed 20% increase in the composite with 0.13% (wt of cement) over the reference after 28 days of curing. Also, the carboxylate MWCNTs with 0.05% (wt of cement) showed 30% increase after 1 day of curing. Thus, the functionalized carbon nanotubes accelerated the cement hydration of Portland cement, thus its early strength. However, the unmodified MWCNTs showed greater compressive strength after 28 days.

2.5 Graphene-cement nanocomposites

The investigation on the effects of graphene and its derivatives on the cement's overall response need multiple approaches from nano-level to micro-level to identify the 3D model of its structure and observe the interactions between graphene and cement matrix.

The graphene nanoparticles are expected to improve the cement matrix in a nanoscale and as well as its micro-scale structure. There has been a lot of research focusing on single wall carbon nanotubes and multiwall carbon nanotubes, as well as on their functionalization and the carbon nanofibers, but little research has been conducted on graphene functionalized with functional groups, which would participate in bonds with the cement oxides. Hence, there is great need for further research to broaden our knowledge on the mechanical, thermal and physical behavior of the graphene-cement nanocomposites.

With respect to previous research studies, graphene embedded to the cement matrix is expected to improve cement's toughness and more specifically its tensile, compressive, bending and interfacial strength. The functionalization of graphene using the remained oxygen atoms of functional groups or grafting the desirable molecules to react with the molecules expected to make the bonds with cement matrix is a new field of interest in the graphene-cement nanocomposites that may change the future of civil engineering applications. Several research studies indicate the significance to investigate further the graphene and its derivatives with cement composites within a holistic approach. It's an issue that requires multi-scale, chemical and atomistic study.

- ➤ Konsta-Gdoutos et al. (2009) used MWCNTs to investigate their reinforcing effect on the cementitious matrix[20]. According to their study, the cementitious matrix showed improved fracture resistance properties. Additionally, the MWCNTs increased the high stiffness of C-S-H gel produced and decreased its porosity. The MWCNTs seem to reduce significantly the capillary stresses because of their small diameters (20-40 nm), thus improving the early strain capacity of the cement nanocomposites. Hence, the MWCNTs cement nanocomposites present early age and long term durability.
- ➤ Babak et al., (2014) investigated the potential of GO to improve the mechanical properties of cement nanocomposites[21]. According to their study 1.5% (wt of cement) GO with 0.5% (wt of cement) superplasticizer showed 48% higher tensile strength compared to the cement matrix without GO. The FE-SEM images showed good bonding between GO and the cement particles. Also, the XRD diffraction data revealed increased amount of C-S-H gel at the cement nanocomposite compared to pure cement mortar.
- ➤ Alkhateb et al. (2013) investigated the effects of functionalized graphene nano-platelets on cement[22]. They simulated the atomic models of G, G(OH), G(NH$_2$), G(COOH) as it can be seen in Figure 6.
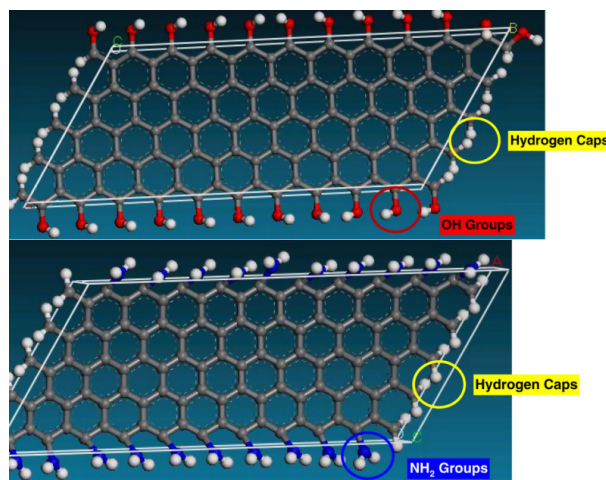

Figure 6 Atomic model of G (OH) and G (NH$_2$) functionalized graphene.

Table 1 presents the interfacial bonding strength calculated as the difference between the

energy of the composite and the individual energies of the composite elements: $\Delta E = E_{total} -$ ($E_{fiber} + E_{matrix}$) and the energy difference was in all cases negative, which means that the compound was energetically favorable. The interaction energy mainly came from the Van der Waals and electrostatic interactions between C-S-H and graphene nano-platelets. The magnitude of the energy difference is defined by the electrostatic energy interactions and the polarity of the functional groups of graphene.

Table 1. The interfacial strength between GCNCs and C-S-H gel

Composite	Interfacial strength (GPa)
(C-S-H)-G()-C-S-H	1.2
(C-S-H)-G(OH)-C-S-H	13.5
(C-S-H)-G(NH2)-C-S-H	6.1
(C-S-H)-G(COOH)-C-S-H	11.8

As it can be seen from the table above the interfacial strength of the G (OH) cement nano-composite was calculated much higher than that only with graphene.

2 EXPERIMENTAL APPROACH AND CHARACTERIZATION METHODS

2.1 Preparation of silica coated GO and silane functionalized GO

GO could be synthesized by following the modified Hummers method. In order to obtain a well-dispersed silica coating layer, tetraalkoxysilane which may be used as the precursor of silica will be added to the GO solution under stirring. After reaction, silica coated GO (noted as GO-SiO$_2$) hybrid sheets were cleaned by repeated washing and centrifugation and re-dispersed into DI water to form homogeneous dispersions. Instead of forming silica coating layer on the surface of GO, the oxygen groups of GO are functionalized with imide and silane groups (noted as FS-GO), which can build covalent bonds with the oxygen groups of GO and C-S-H gel of cement.

2.2 Preparation of cement composites

The cement composite was prepared by mixing 80 g cement, 240 g standard sand with the maximum size of 4 mm, 40 g water, and a certain amount of GO-SiO$_2$ or FS-GO. To be able to uniformly disperse nano-scaled graphene into cement gels, a modified mixing process was developed. Before mixing, the sand was divided into three parts. One part of sand was pre-mixed with cement powder with a high-speed mixer. The rest two parts of sand were mixed with the graphene oxide dispersions with a feed rate of 10 g/min. Then, the pre-mixed cement/sand powder was feed into the above paste to form the final composite. The final paste was molded into a square with a size of 40 mm × 40 mm × 40 mm and de-bubbled with strong vibration. Two specimens were prepared from each mixture for the compressive strength tests. The specimens were demolded after 24 h and then cured in a moist box at room temperature and 95% relative humidity before testing.

2.3 Characterization methods

The morphology of GO-SiO$_2$ was examined using TEM. The microstructure of concrete was analyzed by scanning electron microscopy (SEM). Fourier transform infrared spectroscopy (FT-IR) was carried out to find out functional groups of GO and fGO.

3. RESULTS AND DISCUSSIONS

3.1 Structural characterization of GO nanosheets

GO was exfoliated from pristine graphite by following the Hummer's methods. Significant structural changes occurring during the chemical oxidation process from pristine graphite to GO. The original sp2 domains were partially destroyed and replaced by oxygen groups and defects, which is reflected in the Raman spectrum. As shown in Figure 7, the Raman spectrum of the pristine graphite, as expected, displays a prominent G peak as the only feature at 1581 cm^{-1}, corresponding to the first-order scattering of the E2g mod[23]. In the Raman spectrum of GO, the G band is broadened and shifted to 1594 cm^{-1}. In addition, the D band at 1363 cm^{-1} becomes prominent, indicating increase of defects in the sp2 domain, due to the effects of extensive oxidation. Compared with the spectra of commercial graphene (provided by SHT company), the Raman spectrum of GO shows an increased D/G intensity ratio together with the disappearance of the 2D band. This result also obviously suggests the structural difference of GO with high-quality graphene.
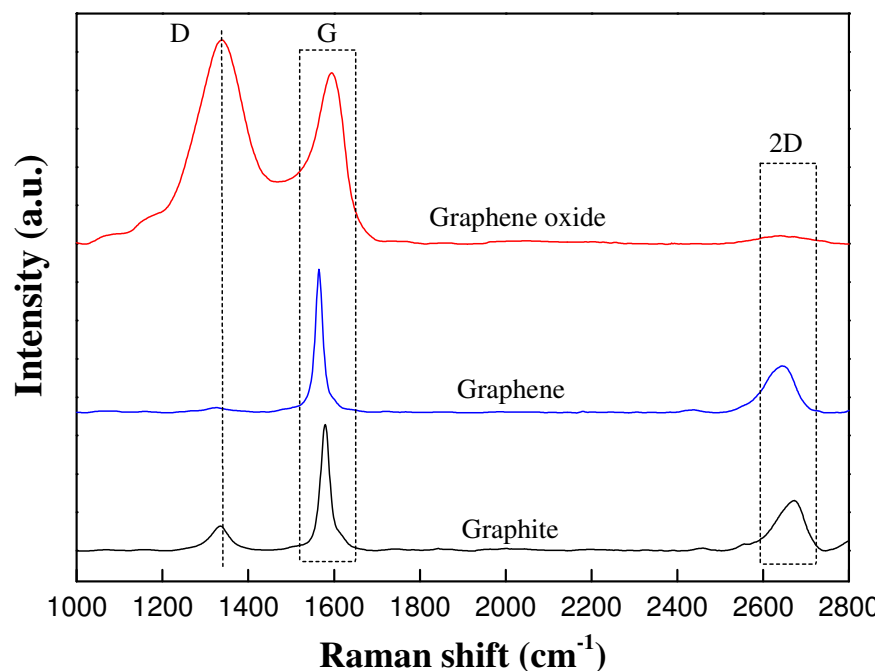

Figure 7 Raman spectrum of GO, commercial graphene and pristine graphite.

The defects and oxygen groups on the surface of GO offer unique properties, such as, GO has a good dispersability in water due to the hydrogen bond formed with water molecules.

Importantly, GO also shows a high reactivity with many functional agents to form various hybrid materials, which offers GO with new properties. These results make GO as a great candidate for cement applications. Here in this project, GO was functionalized with silica to form a coating layer at GO surface. The reason for choosing silica is that amorphous silica can generate abundant Si-OH groups in alkaline condition. These Si-OH groups can quickly react with calcium hydroxide to form complex composites, which would facilitate the fast growth of C-S-H hydrates at the beginning of cement hydration process. Besides that, amorphous silica can increase the contact area of GO with C-S-H hydrates to form densely packed structures around GO and decrease the voids. The FTIR spectra of GO and GO-SiO$_2$ have confirmed the existence of silica. The results are shown in Figure 8. It can be seen that GO has the oxygen groups of -COOH and -O-, supported by the new absorption peaks of GO at 1730 cm^{-1} (-COOH), and 1360 cm^{-1}, 1102 cm^{-1}, 1025 cm^{-1} (-O-). Different from GO spectra, FTIR spectra of GO-SiO$_2$ shows new characteristic bands at 1085, 800 and 460 cm^{-1}, which are correspond to the stretching, bending and out of plane of Si-O bonds respectively. The position and the shape of the main Si-O vibrational band at 1085 cm^{-1} on FTIR spectra shows a stoichiometric silicon dioxide structure.
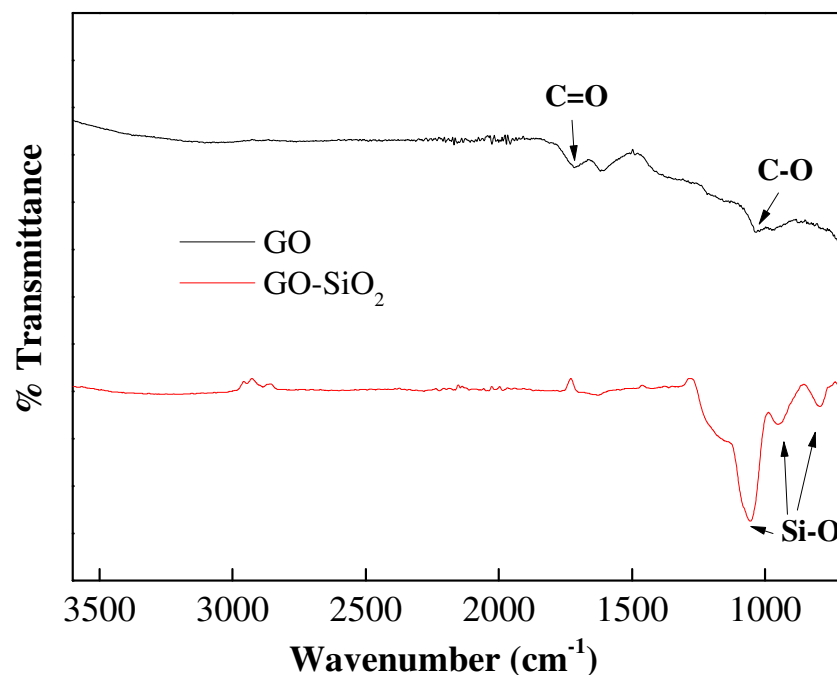

Figure 8 FTIR spectra of GO and GO-SiO$_2$

To give a visual understanding about the morphology difference after silica coating, morphology analysis by TEM was carried out. The results are shown in Figure 9. It can be seen that GO possesses a flexible structure together with folded edges. The average size of GO is about 10 μm, and the number of layers is above than 10 layers. Such a large lateral size and multi-layer structure would offer GO with an improved mechanical strength which can benefit the overall strength of concrete. After coating with silica, an amorphous silica layer was successfully coated on the surface of GO and formed a hybrid composite.
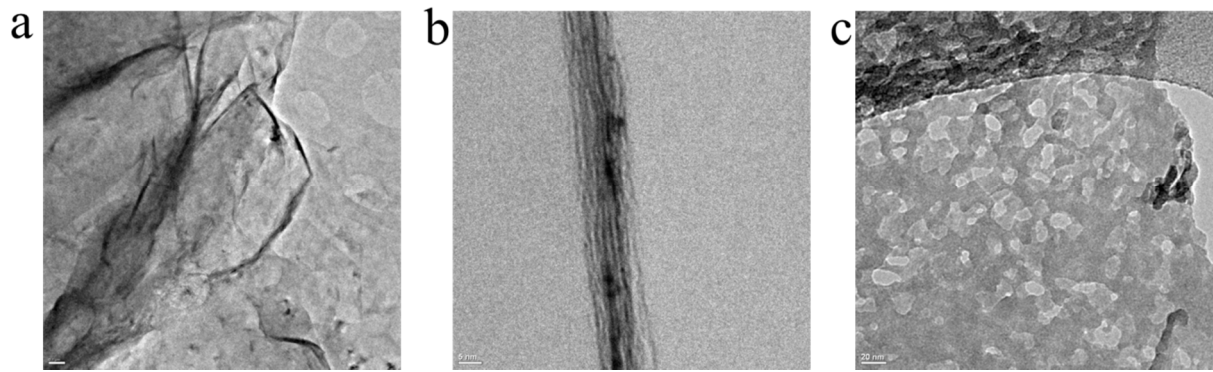
Figure 9 (a,b) TEM images of GO. GO possesses a flexible structure together with folded edges. The average size of GO is about 10 μm, and the number of layers is above than 10 layers.(c) TEM image of GO-SiO$_2$. An amorphous silica layer was successfully coated on the surface of GO and formed a hybrid composite.

3.2 Mechanical strengths

The hybrid composite GO-SiO$_2$, as the reinforcing material, was uniformly mixed into the cement paste. Different samples were fabricated with different adding amounts of GO-SiO$_2$ ($W_{GO-SiO2}$ / W_{cement}). Compressive tests of all samples were carried out after moist cure for 7 days. The results of compressive strength relative to reference are shown in Table 2. It can be seen that the compressive strength of the GO-SiO$_2$ composite decreased with the increasing of weight ratio of GO-SiO$_2$. Compared with the reference, the relative strength of GO-SiO$_2$ composites are 0.92 and 0.86 for different samples with adding amount of 0.1% and 0.68%, respectively. Reasons for such a negative performance of GO-SiO$_2$ are complex. For example, owing to the abundant of Si-OH groups existing on the surface of GO, the hybrid material shows a strong hydrophilic property which can absorb too many water molecules. Without enough water, the workability of cement paste became poor, as observed in the mixing, and the paste tended to form big clusters with loosed connections between each other. Another possible reason is that the silica coating layer could be consumed during the early hydration of cement to form C-S-H hydrates. Once the layer of coated silica was completely reacted, GO would lose connection with the cement and cannot play the reinforcing role in the concrete.

Table 2 Compressive strength of different samples

Sample	Composite						Strength $F_{sample}/F_{reference}$
	Water (g)	Cement (g)	Sand (4mm) (g)	G0-SiO$_2$ (wt%)	GO (wt%)	FS-GO (wt%)	
Reference	40	80	240	-	-	-	1
G0-SiO$_2$1	40	80	240	0.1%	-	-	0.92
G0-SiO$_2$2	40	80	240	0.68%	-	-	0.86
GO1	40	80	240	-	0.15%	-	0.41
GO2	40	80	240	-	0.3%	-	0.42
FS-GO1	40	80	240	-	-	0.15%	1.25
FS-GO2	40	80	240	-	-	0.3%	0.40

To avoid the above mentioned problems, GO was functionalized with amide and silane groups, instead of silica coating layer. Under catalysts, the oxygen groups at the edge of GO would react with the amide and silane groups to form covalent bonds with cement, which are strong enough to combine GO with cement hydrates tightly even after silane groups reacted with cement. This modified GO functional process would have limited effects on the workability of fresh cement paste due to the fact that the functional groups can only form covalent bonds with the oxygen groups at the edge of GO, and combine the GO together with the cement hydrates without significantly absorbing water molecules. This makes the GO playing the reinforcing role in the composite material without impairing the workability of fresh cement paste. The relative values of compressive strength of samples with FS-GO as the reinforcing material are shown in Table 2. It can be seen that the relative strength of the composite was increased to 1.25 with 0.15 wt% of adding amount of FS-GO. However a decrease of relative strength was also observed when the adding amount was increased to 0.3%. Possible reasons for the decrease could be that the addition of too much nanomaterials decreased the workability of the fresh cement paste. To study the reinforcing effect of FS-GO, control experiments with pure GO as the addition material were performed. The results are also shown in Table 2. With the same adding amount of GO, the relative strength of all GO samples shows a dramatic decrease compared with that of FS-GO, which could be caused by lacking connection between GO and cement. Also, the attachment of GO to the surface of cement particles would block the hydration reaction between cement and water, which would hinder the growth of hydrates and bring an adverse effect to the overall strength of concrete.

3.3 Microstructures

To understand the reinforcing mechanism of FS-GO to cement, morphology analysis of different samples were performed by SEM. Figure 10 shows the SEM images of reference sample and FS-GO1 at different magnification ratios. It can be seen that the reference concrete has a porous microstructure with needle-like hydration products (images a, b and c in Figure 10). The mechanical properties and durability of concrete is mainly depended on this needle-like structure. However, the large interspace inside these needle-like hydration products hindered the further improvement of strength and gave the paths to aggressive

substances which impair the durability of concrete. Different from the reference concrete, the sample with a less adding amount of FS-GO (0.15 wt%) shows a much tighter microstructure (images e, f and g in Figure 10). From the SEM images, it can be found that there is almost no void inside the sample. Moreover, the average size of the hydration products is much smaller than that of the reference concrete, which could be caused by the refining effects of FS-GO. With a decreased void ratio, the FS-GO sample demonstrated an improved compressive strength. Therefore, it can be concluded that the covalent bonds between FS-GO and cement can not only form a tight connection but also have an effect of refining the cement microstructure which can reduce the interspace so as to improve both the mechanical strength and the durability of concrete.
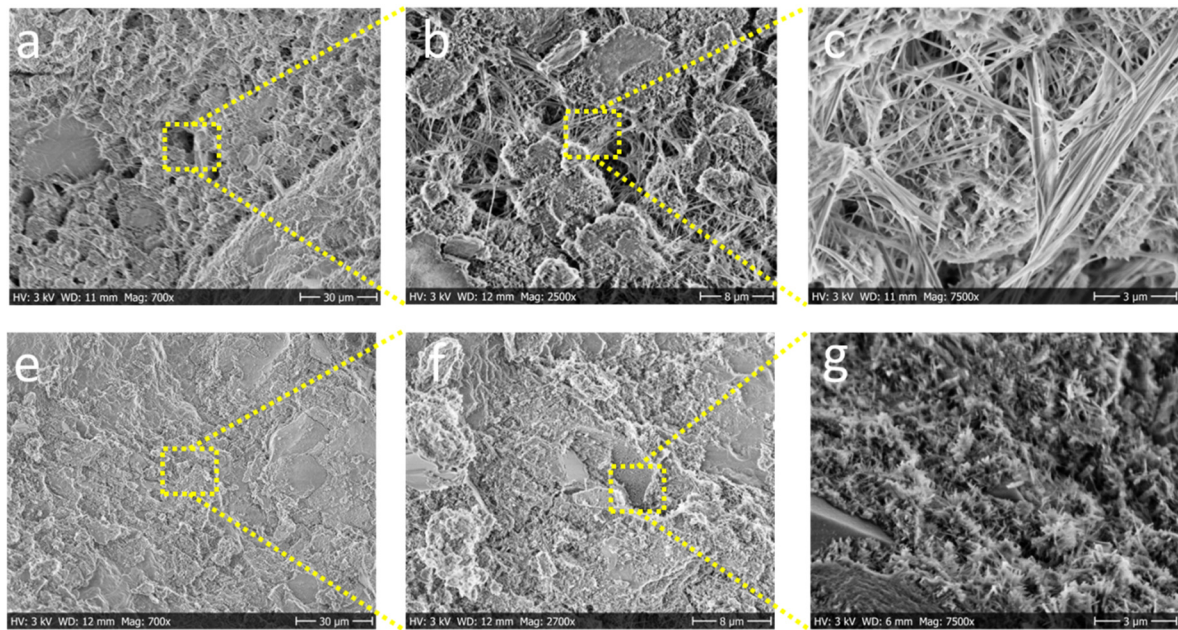

Figure 10 SEM images of microstructure of reference cement sample (a, b and c) and FS-GO1 (e, f and g) with different magnification ratios.

To understand the reason why the compressive strength decreased with increasing of FS-GO weight ratios, the microstructure of samples with 0.3% FS-GO was also analyzed by SEM. The results are shown in Figure 11. It has been found that too much of nanomaterials adding into the cement paste led to a so called island effect. Due to the significantly decrease of workability of fresh cement paste as well as the blocking effect of graphene, the concrete could hold its structure in one piece and turned to form large independent particles with weak connection and large voids between them. This is the major reason for the poor mechanical performance. However, the hydration products inside the FS-GO2 sample show different structures from the reference concrete. Due to the attachment of FS-GO onto the surface of sand and cement particles, large amount of nucleation sites were formed and lead to a fast growth of needle-like hydrates, which show a densely packed structure with a smaller average size compared with the reference concrete. This result indicates that FS-GO can still play the role of refining the cement microstructure. However, the effect of poor workability on the mechanical strength of concrete is much more dominative than the refining effect of the

microstructure. Therefore, it is very important that the addition of nanomaterials should not only refine the microstructure but also have very limited effect on the workability of fresh cement paste.
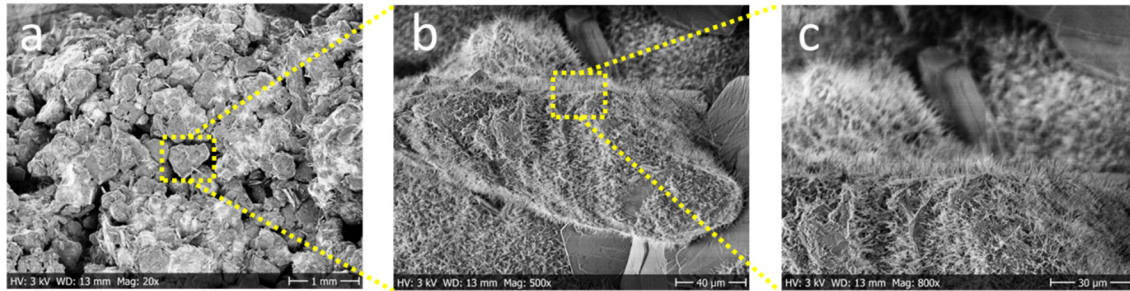

Figure 11 SEM images of microstructure of FS-GO2 with different magnification ratios.

The densities of different samples were also measured and recorded in Table 3. It can be seen that the reference sample has an average density of 2.36 g/cm^3, and the density values of FS-GO1 and FS-GO2 are 2.43 g/cm^3 and 2.25 g/cm^3, respectively. It has been found that the density change shows a similar trend with the mechanical strength change due to the fact that density reflects the effect of voids to the total weight. Therefore, a higher density means a low void ratio and a higher mechanical strength.

Table 3 Density values of standard concrete and sample of FS-GO1 and FS-GO2.

Sample	Reference	FS-GO1	FS-GO2
Density (g/cm^3)	2.36	2.43	2.25

4. CONCLUSIONS AND FUTURE PLANS

In the pre-study the bonds between graphene and cement hydrates were analyzed and two types of functionalized graphene oxides with potential covalent bonds, that is, silica coated GO (GO-SiO$_2$) and silane functionalized GO (FS-GO), were tested. From the results the following conclusions can be drawn.

- Addition of the silica coated GO reveals no improvement of strength probably owing to its high water absorption the silica coated GO which impairs workability of fresh cement paste, resulting in poor compaction of concrete.
- Addition of the silane functionalized GO with 0.15 wt% of cement reveals an increase in compressive strength by 25%, owing to its refinement of microstructures of cement

hydration products. This indicates a promising way to further study of graphene-cement composites.

- The amount of added nanomaterials must be controlled to a level that does not impair the workability of fresh cement paste.

In the future, the adding amount of FS-GO will be optimized to achieve the best performance of cement composite with both mechanical properties and durability. The other potential functional groups will also be investigated, for the improvement of not only cement-based but also asphalt-based binding materials for road constructions.

REFERENCES

1. Yuan, Y. & Ji, Y. Modeling corroded section configuration of steel bar in concrete structure. *Constr. Build. Mater.* **23,** 2461–2466 (2009).
2. Watanabe, K., Kimura, T. & Niwa, J. Synergetic effect of steel fibers and shear-reinforcing bars on the shear-resistance mechanisms of RC linear members. *Constr. Build. Mater.* **24,** 2369–2375 (2010).
3. Hossain, M. Z. & Awal, A. S. M. A. Flexural response of hybrid carbon fiber thin cement composites. *Constr. Build. Mater.* **25,** 670–677 (2011).
4. Reis, J. M. L. Fracture and flexural characterization of natural fiber-reinforced polymer concrete. *Constr. Build. Mater.* **20,** 673–678 (2006).
5. Soroushian, P., Won, J.-P. & Hassan, M. Durability characteristics of CO2-cured cellulose fiber reinforced cement composites. *Constr. Build. Mater.* **34,** 44–53 (2012).
6. Soroushian, P., Tlili, A., Alhozaimy, A. & Khan, A. Development and characterization of hybrid polyethylene-fibre-reinforced cement composites. *Constr. Build. Mater.* **7,** 221–229 (1993).
7. Su, H. & Xu, J. Dynamic compressive behavior of ceramic fiber reinforced concrete under impact load. *Constr. Build. Mater.* **45,** 306–313 (2013).
8. Morova, N. Investigation of usability of basalt fibers in hot mix asphalt concrete. *Constr. Build. Mater.* **47,** 175–180 (2013).
9. Slane, J., Vivanco, J., Meyer, J., Ploeg, H.-L. & Squire, M. Modification of acrylic bone cement with mesoporous silica nanoparticles: Effects on mechanical, fatigue and absorption properties. *J. Mech. Behav. Biomed. Mater.* **29,** 451–461 (2014).
10. Stynoski, P., Mondal, P. & Marsh, C. Effects of silica additives on fracture properties of carbon nanotube and carbon fiber reinforced Portland cement mortar. *Cem. Concr. Compos.* **55,** 232–240 (2015).
11. Pan, Z. *et al.* Mechanical properties and microstructure of a graphene oxide-cement composite. *Cem. Concr. Compos.* doi:10.1016/j.cemconcomp.2015.02.001
12. Pellenq, R. J.-M., Lequeux, N. & van Damme, H. Engineering the bonding scheme in C–S–H: The iono-covalent framework. *Cem. Concr. Res.* **38,** 159–174 (2008).
13. Manzano, H., Dolado, J. S., Guerrero, A. & Ayuela, A. Mechanical properties of crystalline calcium-silicate-hydrates: comparison with cementitious C-S-H gels. *Phys. Status Solidi A* **204,** 1775–1780 (2007).
14. Chen, Q. Y., Tyrer, M., Hills, C. D., Yang, X. M. & Carey, P. Immobilisation of heavy

metal in cement-based solidification/stabilisation: A review. *Waste Manag.* **29,** 390–403 (2009).

15. Richardson, I. G. The nature of C-S-H in hardened cements. *Cem. Concr. Res.* **29,** 1131–1147 (1999).

16. Geim, A. K. & Novoselov, K. S. The rise of graphene. *Nat. Mater.* **6,** 183–191 (2007).

17. Warner, J. H. *et al.* Structural transformations in graphene studied with high spatial and temporal resolution. *Nat. Nanotechnol.* **4,** 500–504 (2009).

18. Dikin, D. A. *et al.* Preparation and characterization of graphene oxide paper. *Nature* **448,** 457–460 (2007).

19. Bolshakov, V. I., Petrunin, S. & Vaganov, V. Study of features of hydration grained concrete modified with carbon nanotubes. *Bull. Pridniprovsk State Acad. Civ. Eng. Archit.* **0,** 10–20 (2013).

20. Konsta-Gdoutos, M. S., Metaxa, Z. S. & Shah, S. P. Highly dispersed carbon nanotube reinforced cement based materials. *Cem. Concr. Res.* **40,** 1052–1059 (2010).

21. Babak, F., Abolfazl, H., Alimorad, R. & Parviz, G. Preparation and Mechanical Properties of Graphene Oxide: Cement Nanocomposites. *Sci. World J.* **2014,** e276323 (2014).

22. Materials Genome for Graphene-Cement Nanocomposites. *J. Nanomechanics Micromechanics* **3,** 67–77 (2013).

23. Gupta, A., Chen, G., Joshi, P., Tadigadapa, S. & Eklund. Raman Scattering from High-Frequency Phonons in Supported n-Graphene Layer Films. *Nano Lett.* **6,** 2667–2673 (2006)

24. Bentz, D.P.; Cement and Concrete Research. 38, 196–204 (2008)

25. Newman J.W. In: International SAMPE Symposium Exhibition, vol. 32, SAMPE, Covina, CA, 938-944 (1987).